Excited-State Dynamics of Organic Radical Ions in Liquids and in Low-Temperature Matrices

Pierre Brodard,[†] Alexandre Sarbach,[‡] Jean-Claude Gumy,[§] Thomas Bally, and Eric Vauthey*,[†]

Institut de Chimie-Physique de l'Université de Fribourg, Pérolles, CH-1700 Fribourg, Switzerland

Received: March 1, 2001; In Final Form: April 25, 2001

The excited-state dynamics of the radical cations of perylene ($PE^{\bullet+}$), tetracene ($TE^{\bullet+}$), and thianthrene ($TH^{\bullet+}$), as well as the radical anions of anthraquinone ($AQ^{\bullet-}$) and tetracenequinone ($TQ^{\bullet-}$), formed by γ irradiation in low-temperature matrices ($PE^{\bullet+}$, $TH^{\bullet+}$, $AQ^{\bullet-}$, and $TQ^{\bullet-}$) or by oxidation in sulfuric acid ($PE^{\bullet+}$, $TE^{\bullet+}$, and $TH^{\bullet+}$) have been investigated using ultrafast pump−probe spectroscopy. The longest ground-state recovery time measured was 100 ps. The excited-state lifetime of $PE^{\bullet+}$ is substantially longer in low-temperature matrices than in H_2SO_4, where the effects of perdeuteration and of temperature on the ground-state recovery dynamics indicate that internal conversion is not the major decay channel of $PE^{\bullet+}$*. The data suggest that both $PE^{\bullet+}$* and $TE^{\bullet+}$* decay mainly through an intermolecular quenching process, most probably a reversible charge transfer reaction. Contrarily to $AQ^{\bullet-}$*, $TQ^{\bullet-}$* exhibits an emission in the visible which, according to theoretical calculations, occurs from an upper excited state.

Introduction

Although photoinduced electron transfer (ET) reactions have been very extensively investigated,[1] the excited-state properties of the reaction products, open-shell radical ions, are much less documented. This is rather surprising, because excited radical ions have been invoked to account for phenomena as diverse as the absence of the inverted region in very exergonic ET quenching reactions[2] or the emissive diffuse interstellar bands.[3] Moreover, photoexcited radical cations seem to be efficient redox catalysts.[4,5] A major reason for the lack of information on these species is certainly the absence of fluorescence from most radical ions in the condensed phase, as opposed to the gas phase, where several classes of organic radical cations have been found to fluoresce.[6,7] As shown by Breslin and Fox,[8] many emissions ascribed to radical ions are in fact due to secondary closed-shell products. There are indeed only few reports of genuine emission from excited radical ions in the condensed phase.[9−15] The very small fluorescence quantum yield of radical ions seems to be due to the combination of two effects: (1) fast nonradiative deactivation from the lowest doublet excited state and (2) a small radiative rate constant for the D_1-D_0 transition. Indeed, many radical ions show very weak D_0-D_1 transitions. Moreover, the corresponding emissions are, in most cases, in the near-IR spectral region, and hence difficult to detect.

We have recently reported an investigation of the excited-state lifetime of a few radical cations (perylene cation, $PE^{\bullet+}$) and anions ($PE^{\bullet-}$ and anthraquinone anion, $AQ^{\bullet-}$) in the condensed phase, using the transient grating technique.[16] It was found that in liquids, the decay times are below 15−25 ps, the time resolution of the experiment. On the other hand, the excited-state lifetime of $PE^{\bullet+}$ in boric acid glass amounts to 35 ps. In view of the small D_1-D_0 energy gap of $PE^{\bullet+}$ (1.5 eV), these decay times are surprisingly short for an internal conversion (IC). IC in rigid closed-shell molecules with similar energy gaps is usually slower. For example, the excited lifetime of the dye IR140, with a S_1-S_0 gap of 1.45 eV, is 700 ps.[17] In some cases, however, suitably positioned conical intersections of the S_1 and S_0 potential surfaces may strongly accelerate IC.[18] For example, the lifetime of azulene in the S_1 state, which lies about 1.75 eV above S_0, varies from 1.7 ps, when excited in the 0−0 transition, to 400 fs, when excited with 0.16 eV excess energy.[19] This dependence of the lifetime on the vibrational excess energy is in agreement with a conical intersection located above the S_1 minimum.[20]

CHART 1

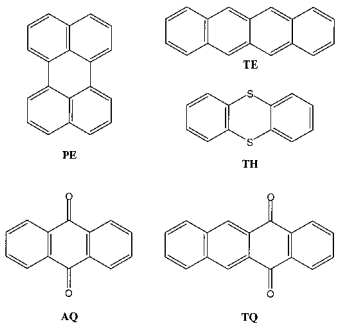

We report here on a detailed investigation of the excited-state dynamics of radical cations and radical anions (see Chart 1) formed by γ irradiation in low-temperature matrices or by oxidation in concentrated sulfuric acid, using the transient grating technique (TG) and transient absorption (TA). In sulfuric acid, we have investigated the effect of deuteration of both the solute and the solvent and of temperature on the excited lifetime of $PE^{\bullet+}$. Finally, we also report on the observation of an emission from $TQ^{\bullet-}$* in a rigid matrix at 77 K. According to ab initio calculations, this fluorescence takes place from an upper excited state.

* Corresponding author. Email: Eric.Vauthey@chiphy.unige.ch.

[†] Present address: Department of Physical Chemistry, University of Geneva, Quai Ernest Ansermet 30, CH-1211 Genève 4, Switzerland.

[‡] Present address: Institut de Physique, Allée du 6 août, 4000-Sart-Tilman Liège, Belgique.

[§] Present address: Department of Chemistry 0358, University of California, San Diego, 9500 Gilman Dr., La Jolla, CA 92093.

10.1021/jp010808l CCC: $20.00
Published on Web 06/16/2001

Experimental Section

TG Setups. Two different TG setups, depending on the excitation wavelength (532 or 840 nm), have been used. The TG setup for 532 nm excitation has been described in detail in ref 16. Briefly, the second harmonic output of a passive/active mode-locked Nd:YAG laser (Continuum PY61-10) was split into three pulses. Two time coincident pulses of equal intensity were crossed on the sample to generate the grating. Unless specified, the crossing angle θ_{pu} was 1°. The third pulse was sent along an optical delay line before striking the grating in a BOXCARS geometry. The total energy of the pump pulses was about 40 μJ and that of the probe pulse about 20 times smaller. The beam diameters on the sample were around 1.5 mm and the pulse duration was about 25 ps. The polarization of the probe pulse was at magic angle relative to that of the pump pulses. To record transient spectra, multiplex TG was performed.[21−23] In this case, the probe pulse was obtained by supercontinuum generation in a H_2O/D_2O mixture. The diffracted pulse, containing the TG spectrum, was sent into a spectrometer equipped with a CCD camera.

Excitation at 840 nm was performed by two time coincident laser pulses, crossing the sample with an angle of 1.2°.[24] These pulses were produced by a standard 1 kHz amplified Ti:Sapphire system (Spectra-Physics). The duration of the pulses was about 120 fs and the pump energy on the sample was around 10 μJ with a spot size of 1.5 mm diameter. For probing, a weaker and time delayed pulse at the same wavelength was used. BOXCARS geometry and magic angle polarization were also applied. The diffracted pulse was sent to a photomultiplier tube, whose output was connected to a computer board for digitization (Axiom AX5210A/D board). For multiplex TG, white light obtained by focusing the 840 nm pulses in a H_2O/D_2O mixture was used. Detection was performed as described above for the 532 nm setup. The resulting TG spectra were corrected for the chirp of the probe pulse as described in ref 25.

TA Setup. the same laser as described above in the 532 nm TG setup was used. The pump energy on the sample was around 0.5 mJ with a spotsize of 1.5 mm diameter. The absorbance was probed at the same wavelength using magic angle polarization.

Fluorescence. Fluorescence spectra were recorded using a CCD camera (Oriel Instaspec IV) connected to a $^1/_4$ m imaging spectrograph (Oriel Multispec 257). All spectra were corrected for the spectral sensitivity of the CCD camera. Excitation was performed between 500 and 620 nm with a broadband OPO (GWU OPO−C-355) pumped by the third harmonic output of a Q-switched Nd:YAG laser (Continuum, Surelite II-10). The pulse energy in this wavelength range was kept constant at about 1 mJ. Fluorescence lifetimes were measured using the 25 ps pulses at 532 nm for excitation. Detection was achieved with a fast PIN silicon photodiode (Motorola MRD 500) connected to a 500 MHz, 2 GS/s digital oscilloscope (Tektronik TDS-620A). The response function of this system had a fwhm of about 850 ps.

Data Analysis. The time profiles of the TA and TG intensity were analyzed by iterative reconvolution using eq 1:

$$I_s(t) = \int_{-\infty}^{+\infty} I_{pr}(t - t'')[\int_{-\infty}^{t} S(t' - t)I_{pu}(t')\,dt']^n\,dt'' \quad (1)$$

where $n = 1$ for TA and $n = 2$ for TG. I_{pu} and I_{pr} are the intensities of the pump and probe pulses, respectively, and S is the response of the sample. The integral in square bracket is the convolution of the sample response with the pump pulse, whereas the first integral is the convolution with the probe pulse.

Samples. Anthraquinone (AQ) and thianthrene (TH) were recrystallized, while 1,4-diazabicyclo[2.2.2]octane (DABCO), perylene (PE), perylene-d_{12} (PEd, Cambridge Isotopes), tetracene (TE), and 5,12-tetracenequinone (TQ) were vacuum sublimed. Tetrahydrofuran (THF, UV grade) was dried as described in ref 26. Trichlorofluoromethane (F11), 1,2-dibromotetrafluoroethane (F114B2, Fluorochem), *n*-butyl chloride (BuCl), isopentane (iPe), and 2-methyltetrahydrofuran (MTHF) were distilled. Sulfuric acid (95−97%, Merck, pro analysis), deuterated sulfuric acid (96−98% in D_2O, Cambridge Isotopes), and acetonitrile (ACN, UV grade) were used without further purification. Unless specified, all compounds were from Fluka.

For preparing radical cations in rigid matrices, 10^{-2}−10^{-3} M solutions of the neutral precursors were prepared either in a 50/50 mixture of iPe and BuCl or in a 50/50 mixture of Freons F11 ($CFCl_3$) and F114B2 (CF_2BrCF_2Br).[27] For making radical anions, the neutral precursors were dissolved in MTHF.[27] About 1 mL of these solutions was then transferred into a home-built cell comprising two 1 mm thick quartz windows separated by a gap of 1 mm. After immersion in liquid nitrogen (LN_2), glasses of fair optical quality were obtained. These glasses were exposed to the γ radiation produced by a ^{60}Co source (Gammacell 220 MDS Nordian Inc.). In the case of MTHF, the irradiated glasses were briefly illuminated with >700 nm light in order to remove a broad absorption band centered around 1300 nm due to the trapped electrons. For spectroscopic measurements, the samples were placed in a home-built LN_2 immersion cryostat.[28] The sample head was designed to minimize the optical path length in LN_2 to less than 1 mm. The absorbance of the sample at the probe wavelength was around 0.2.

In sulfuric acid, $PE^{\bullet+}$, $TE^{\bullet+}$, and $TH^{\bullet+}$ were readily prepared by adding the corresponding neutral compound to the acid. The concentration was kept below 10^{-4} M, to avoid the formation of the dimers.[29,30] For TG measurements at 840 nm, the sample solutions were placed in a home-built rotating cell with an optical path length of 1 mm.[24] The absorbance at 840 nm was around 0.2. For TA measurement at 532 nm, a 1 cm cell was used and the absorbance at 532 nm was around 1. During the measurement, the samples were continuously stirred by N_2 bubbling. No significant sample degradation was observed after the measurements.

Computation. The geometry of $TQ^{\bullet-}$ was optimized by the UB3LYP density functional method[31,32] as implemented in the Gaussian 98 suite of programs,[33,34] using the 6-31G* basis set. Excited states were calculated at this geometry by a recently introduced molecular density functional method based on time-dependent (TD) response theory.[35] We used the TD-DFT implementation in Gaussian 98[33] as described recently by Stratmann et al.,[36,37] again together with the 6-31G* basis set.

Results and Discussion

Radical Cations. Figure 1 shows the steady state absorption spectra of solutions of PE, TE, and TH in sulfuric acid. These spectra can be unambiguously ascribed to the radical cations, $PE^{\bullet+}$, $TE^{\bullet+}$, and $TH^{\bullet+}$, respectively.[38] The absorption spectrum of a fresh solution of TE in H_2SO_4 exhibits additionally a band centered at 460 nm due to protonated tetracene, TEH^+.[39] After a few hours, this band vanishes spontaneously and the absorption spectrum is that of $TE^{\bullet+}$ only. The excited-state lifetimes of $PE^{\bullet+}$ and $TH^{\bullet+}$ were determined by performing ground-state recovery (GSR) measurements at 532 nm (cf. arrows in Figure 1), i.e., by exciting in the strong absorption bands corresponding to the D_0−D_5 and D_0−D_3 transition of $PE^{\bullet+}$ and $TH^{\bullet+}$, respectively.[9,40] Figure 2A shows the time profile of the

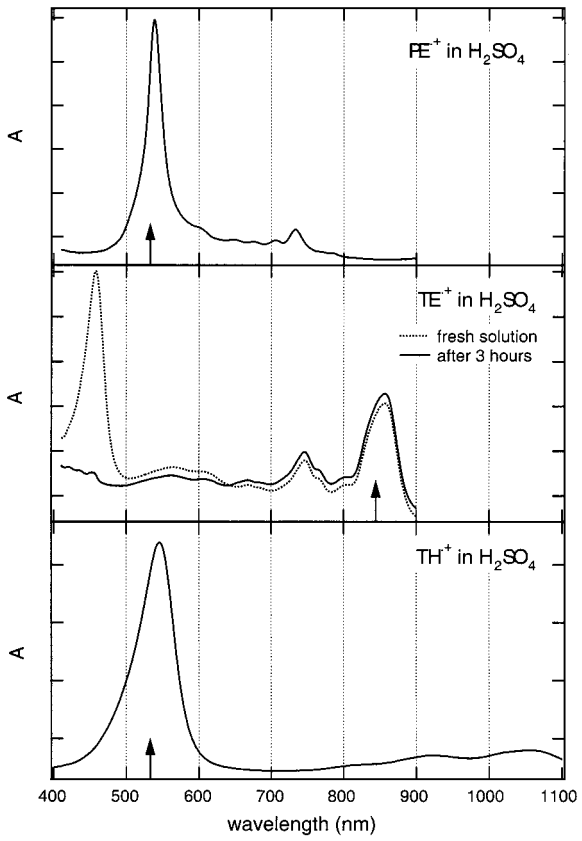

Figure 1. Absorption spectra of $PE^{\bullet+}$, $TE^{\bullet+}$, and $TH^{\bullet+}$ in concentrated sulfuric acid (small arrows: pump and probe wavelength).

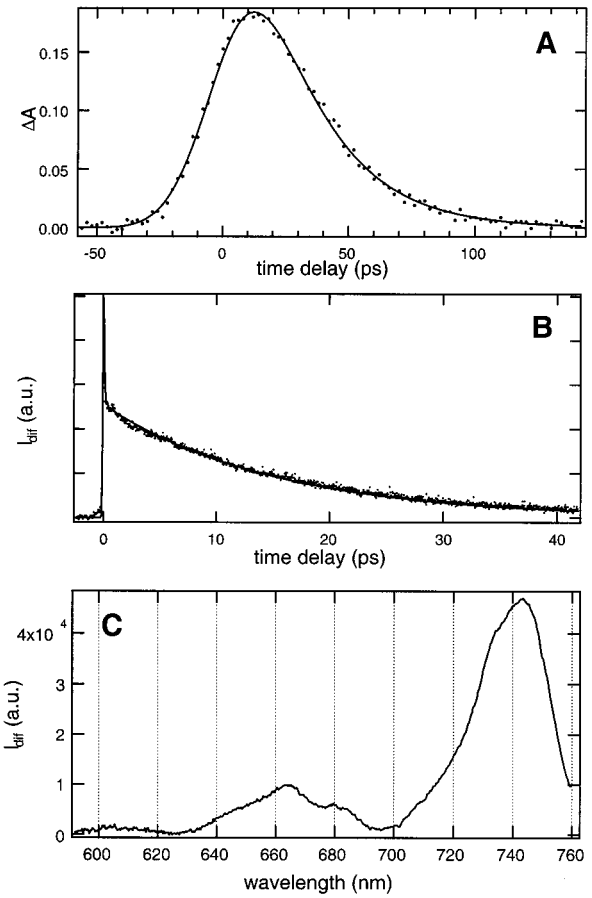

Figure 2. (A) Time profile of the change of absorbance at 532 nm after excitation of $PE^{\bullet+}$ in H_2SO_4. (B) Time profile of the diffracted intensity at 840 nm measured with $TE^{\bullet+}$ in H_2SO_4 (solid lines: best fits of eq 1). (C) TG spectrum measured 2 ps after excitation at 840 nm of $TE^{\bullet+}$ in H_2SO_4.

absorbance at 532 nm after excitation of $PE^{\bullet+}$ at the same wavelength. The GSR is very fast, close to the pulse duration. The solid line is the best fit of eq 1 with an exponential function for the sample response. The resulting decay time amounts to 26 ps for $PE^{\bullet+}$ and 25 ps for $TH^{\bullet+}$ (see Table 1). Multiplex TG measurements have also been performed with $PE^{\bullet+}$ in sulfuric acid. The resulting TG spectra do not exhibit any band that could be ascribed to $PE^{\bullet+}$* or to another transient. Although the signal-to-noise ratio was better in the TG than in the TA measurements, the GSR time constant could not be determined as reliably from the time profile of the TG intensity. The TG intensity is proportional to the square of the concentration changes,[41] and if these changes follow exponential kinetics, the TG intensity decays twice as fast as the TA intensity. Therefore, the TG time profile of $PE^{\bullet+}$ in H_2SO_4 should decay with a time constant of about 13 ps, i.e., within the pulse duration. This problem of time resolution is no longer present when using 840 nm pulses, which have a duration of 120 fs. Figure 2B shows the time profile of the TG intensity, also called diffracted intensity I_{dif} at 840 nm after excitation at the same wavelength of a solution of $TE^{\bullet+}$ in H_2SO_4. The solid line is the best fit of eq 1 with two exponential and one Gaussian functions for the sample response. The Gaussian and one exponential are used to reproduce the first few 100 fs of the TG decay, where a spectral hole-burning effect[17,42,43] and the nonresonant response of the solvent[44] dominate. The second exponential accounts for the slow decay of the signal due to the GSR of $TE^{\bullet+}$. The resulting GSR time of $TE^{\bullet+}$, hence the lifetime of $TE^{\bullet+}$* was found to amount to 26 ps, a value very similar to those found for $PE^{\bullet+}$* and $TH^{\bullet+}$*.

Figure 2C shows the TG spectrum measured 2 ps after excitation at 840 nm of $TE^{\bullet+}$ in H_2SO_4. As explained in detail elsewhere,[21,45] a TG spectrum is very similar to a TA spectrum, the major difference being that the TG intensity is always positive. Thus, the TG band at 745 nm is due to the *bleaching* of $TE^{\bullet+}$ in the ground state. This band decays upon GSR, similarly to the time profile shown in Figure 2B. The smaller TG band centered at 663 nm is not related to ground-state bleaching, because the absorption spectrum of $TE^{\bullet+}$ does not have any band in this region (see Figure 1B). As it has essentially the same time dependence as the 750 nm band, this 663 nm band is most probably due to *absorption* of $TE^{\bullet+}$*.

TABLE 1: GSR Time Constants τ_{GSR} of Radical Ions in Various Media

ion	medium	τ_{GSR} (ps)
$PE^{\bullet+}$	H_2SO_4	26
$PE^{\bullet+}$	D_2SO_4	30
$PEd^{\bullet+}$	H_2SO_4	32
$PEd^{\bullet+}$	D_2SO_4	38
$PE^{\bullet+}$	Freon glass	100
$PE^{\bullet+}$	iPe/BuCl glass	83
$TE^{\bullet+}$	H_2SO_4	26
$TE^{\bullet+}$	D_2SO_4	30
$TH^{\bullet+}$	H_2SO_4	25
$TH^{\bullet+}$	D_2SO_4	25
$TH^{\bullet+}$	iPe/BuCl glass	33
$TQ^{\bullet-}$	ACN	<20
$AQ^{\bullet-}$	MTHF glass	71

$PE^{\bullet+}$ and $TH^{\bullet+}$ were also generated by γ irradiation in solid matrices at 77 K. Their absorption spectra are identical to those reported in the literature.[38] Figure 3 shows the GSR dynamics of $PE^{\bullet+}$ in a Freon glass and of $TH^{\bullet+}$ in an iPe/BuCl glass measured by TG. The GSR dynamics of $PE^{\bullet+}$ and hence the lifetime of $PE^{\bullet+}$* is more than three times longer than in H_2SO_4,

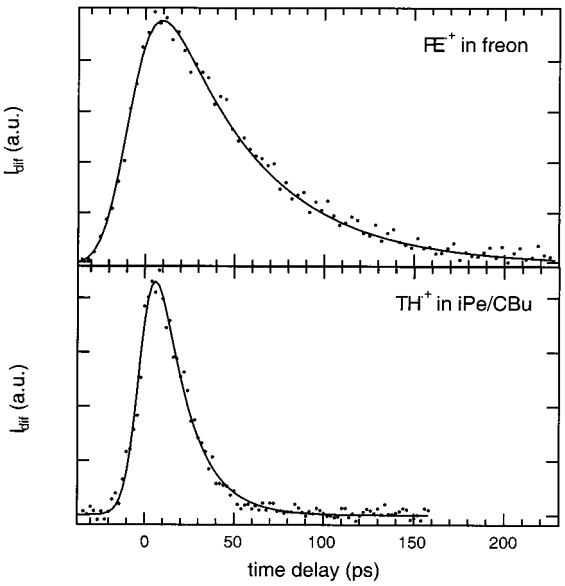

Figure 3. Time profiles of the diffracted intensity at 532 nm measured with $PE^{\bullet+}$ and $TH^{\bullet+}$ in low-temperature matrices after excitation at 532 nm and best fits of eq 1 (solid lines).

while that of $TH^{\bullet+}$ is close to that measured in H_2SO_4 (see Table 1). In both cases, the GSR is complete, indicating no significant photobleaching of the cation population.

The emission of $PE^{\bullet+}$* in low-temperature matrices has already been reported [9] and no attempt was made here to observe it. In the case of $TH^{\bullet+}$, no emission could be found in the visible region, even upon laser excitation. The absence of fluorescence from $TH^{\bullet+}$* in the visible can be easily explained by the fact that the intense 550 nm absorption band corresponds to the D_0-D_3 transition of $TH^{\bullet+}$, the D_2 and D_1 states being responsible for the weak near-IR bands around 800 and 1050 nm, respectively.[40] The D_3-D_2 energy gap is thus certainly too narrow for emission from D_3 to compete with IC to D_2. Consequently fluorescence from $TH^{\bullet+}$* should be looked for in the near-IR. The natural fluorescence lifetime τ_{rad} can be calculated from the oscillator strength f using the following equation:

$$\tau_{rad} = \frac{\epsilon_0 m_e c^3}{2\pi e^2 \nu^2 n^3} f^{-1} \qquad (2)$$

where e is the elementary charge, ν the average emission frequency, ϵ_0 the vacuum permittivity, m_e the mass of the electron, c the velocity of light in vacuum, and n the refractive index of the medium. Using a $f = 0.06$ for the D_0-D_1 transition,[40] this equation predicts a natural fluorescence lifetime of 135 ns for $TH^{\bullet+}$*. On the other hand, the time constant for IC can be estimated from the following equation:[46]

$$\tau_{IC} \approx 10^{-13}\, s^{-1} \exp[\alpha \Delta E] \qquad (3)$$

where ΔE is the energy gap between the two electronic states and where α is of the order of 5 eV^{-1} for rigid aromatic hydrocarbons.[47] With this equation, $\tau_{IC} = 30$ ps is obtained for the D_1-D_0 transition of $TH^{\bullet+}$. With this value, which is in agreement with the measured GSR time constant, and with τ_{rad} determined above, the fluorescence quantum yield of $TH^{\bullet+}$* is predicted to be of the order of 2×10^{-5}!

Table 1 shows that the medium has a strong influence on the lifetime of $PE^{\bullet+}$*. If the decay of $PE^{\bullet+}$* is essentially by IC, this medium effect could be due to a slow down of the vibrational relaxation on going from liquids to solids matrices.

TABLE 2: Activation Energies, E_a in meV, Associated with the GSR Dynamics of $PE^{\bullet+}$ in Sulfuric Acid

ion/medium	H_2SO_4	D_2SO_4
$PE^{\bullet+}$	41 ± 8	54 ± 8
$PEd^{\bullet+}$	66 ± 9	78 ± 12

Vibrational relaxation is involved in two steps: (1) in the relaxation to the lowest excited state, D_1, after excitation at 532 nm and (2) in the transition from D_1 to the ground state. About 0.8 eV are released in the first step and twice as much in the second step. If vibrational relaxation is slower in the solid matrices, the cooling of the hot ground state should show itself in the GSR dynamics of $PE^{\bullet+}$. Indeed, the GSR should be biphasic, with a fast component corresponding to the population of $PE^{\bullet+}(D_0, \upsilon \neq 0)$ and a slower one due to the cooling to $PE^{\bullet+}(D_0, \upsilon = 0)$.[48-50] The observed monoexponential GSR dynamics seems to indicate that vibrational relaxation is not responsible for the longer GSR times observed in low-temperature matrices. IC being essentially a tunneling process, it is independent of temperature. Consequently, if $PE^{\bullet+}$* decays by IC, temperature cannot be invoked to account for the slow GSR measured at 77 K.

To examine whether $PE^{\bullet+}$* truly decays by IC, the GSR measurements were repeated with $PEd^{\bullet+}$ in H_2SO_4. Table 1 shows that the GSR of $PEd^{\bullet+}$ is indeed slower than that of $PE^{\bullet+}$. However, the observed isotope effect is very small. The ratio of the time constants times τ_D/τ_H is 1.23, i.e., much smaller than that reported for the T_1-S_0 radiationless transition of aromatic hydrocarbons. Siebrand and Williams have shown that, in this case, the magnitude of the isotope effect depends on the energy gap between the two electronic states involved in the transition and on the relative number of H atoms in the molecule.[51] Using the isotope rule derived by these authors, an isotope effect τ_D/τ_H of more than 5 is predicted for the IC between two states with the D_1-D_0 energy gap of $PE^{\bullet+}$. Moreover, eq 3 predicts an IC time constant of 200 ps, which is of the same order of magnitude as the GSR time constant in low-temperature matrices but substantially larger than that measured in sulfuric acid.

These discrepancies can be interpreted in two different ways: 1) IC is not the main deactivation pathway of $PE^{\bullet+}$* or 2) the C−H vibrational modes do not participate in the IC. This second hypothesis is rather improbable, because there is no obvious reason why the role of C−H vibrations should be fundamentally different in D_1-D_0 and in T_1-S_0 transitions of planar aromatic hydrocarbons. On the other hand, the first hypothesis is substantiated by the deuterium effect of sulfuric acid. As shown in Table 1, going from H_2SO_4 to D_2SO_4 has about the same effect on τ_{GSR} as perdeuteration of $PE^{\bullet+}$. The GSR time constant of $TE^{\bullet+}$ increases similarly upon perdeuteration of sulfuric acid, while that of $TH^{\bullet+}$ remains constant. The deuterium effects of the solute and of the solvent are roughly additive, the slowest GSR being measured with $PEd^{\bullet+}$ in D_2SO_4.

The above observations indicate that the observed GSR retardations are probably due to kinetic isotope effects for a bimolecular reaction between $PE^{\bullet+}$* and sulfuric acid. This is confirmed by the temperature dependence of the GSR time constant of $PE^{\bullet+}$ and $PEd^{\bullet+}$ in both H_2SO_4 and D_2SO_4. The GSR rate constants exhibit an Arrhenius-type temperature dependence with an activation energy that increases with the amount of deuterium substitution (see Table 2). The variation of τ_{GSR} of $TE^{\bullet+}$ by going from H_2SO_4 to D_2SO_4, together with a calculated IC time constant of 130 ps suggest that the decay of $TE^{\bullet+}$* is also dominated by a similar quenching process. On

the other hand, the GSR time constant of $TH^{\bullet+}$ is independent of the deuteration of sulfuric acid and is about the same in this medium as in the low-temperature glass. Moreover, the GSR time agrees well with the IC time constant estimated with eq 3. This strongly suggests that, contrarily to $PE^{\bullet+}$* and $TE^{\bullet+}$*, IC is the main deactivation pathway of $TH^{\bullet+}$*.

Shkrob et al. have shown that *hole injection* is a general deactivation mechanism of excited aromatic radical cations, both in polar and non polar liquids.[52] Thereby, an electron is transferred from the solvent to the excited cation to produce the neutral molecule in its ground state. This reaction takes place in all solvents, except those with a high ionization potential like acetonitrile (ACN) or sulfuric acid. Moreover, in the latter, the radical cations of aromatic hydrocarbons are thermodynamically more stable than the neutrals.

The observation of a deuterium isotope effect and of the related increase of the activation energy for GSR indicate that the reaction responsible for the deactivation of $PE^{\bullet+}$* and $TE^{\bullet+}$* most probably involves a proton, a hydrogen atom or an electron transfer. Protonated PE, PEH^+, is known to be present at low concentration in sulfuric acid.[53] Similarly, the absorption of TEH^+ can be clearly observed in the spectrum of a fresh solution of TE in sulfuric acid, but it disappears after a few hours. Both PEH^+ and TEH^+, which are formed in a dark reaction, are thus relatively stable species in sulfuric acid, and they may therefore also be formed by H abstraction of $PE^{\bullet+}$* and $TE^{\bullet+}$* from H_2SO_4. As PEH^+ and TEH^+ do not absorb at the probe wavelength, their formation upon reaction of $PE^{\bullet+}$* and $TE^{\bullet+}$* would manifest itself as an incomplete recovery of the ground-state absorbance. Moreover, the formation of the protonated species should be visible in the TG spectra. As the GSR of $PE^{\bullet+}$ and $TE^{\bullet+}$ in sulfuric acid is complete, and as PEH^+ and TEH^+ are not detected in the TG spectra, this process can be safely ruled out.

Reversible proton transfer is another reaction that may account for the fast decay of $PE^{\bullet+}$* and $TE^{\bullet+}$* in H_2SO_4. Proton exchange reactions are known to be responsible for the quenching of excited neutral aromatic hydrocarbons in acidic solutions.[54,55] The isotope effects observed for such processes are of the same order of magnitude than those measured here and the activation energies are also very small. In the present case, the reaction products would correspond to protonated cations (PEH^{2+} and TEH^{2+}) that would be expected to deprotonate very rapidly and give the ground state radical cation. Such a mechanism might also be at the origin of the relatively short lifetime of $PE^{\bullet+}$* in boric acid glass.[16] However, we have shown that the excited-state lifetime of $PE^{\bullet+}$ generated by photoinduced electron transfer between PE* and tetracyanoethylene (TCNE) in ACN was shorter than about 15−20 ps. In this case, the fast decay is certainly not due to a proton exchange reaction with the solvent and must be due to some other process. Moreover, such a reaction does not account for the isotope effect on going from PE to PEd.

Finally, the occurrence of an electron transfer (ET) reaction as a quenching mechanism should also be considered. Given the high ionization potential of sulfuric acid,[56] the medium would certainly act as electron acceptor in such a reaction. Moreover, the resulting ion pair ($H_2SO_4^{\bullet-}/PE^{2+}$) enjoys much better solvation than the product of the opposite ET, i.e., $H_2SO_4^{\bullet+}$/PE. The dications PE^{2+} and TE^{2+}, which can be prepared upon oxidation by SbF_5 in H_2SO_4,[57] have intense absorption bands at 512 and 651 nm, respectively. The absence of any transient in the TG spectra of $PE^{\bullet+}$ in H_2SO_4 mentioned above does however not rule out the occurrence of the above

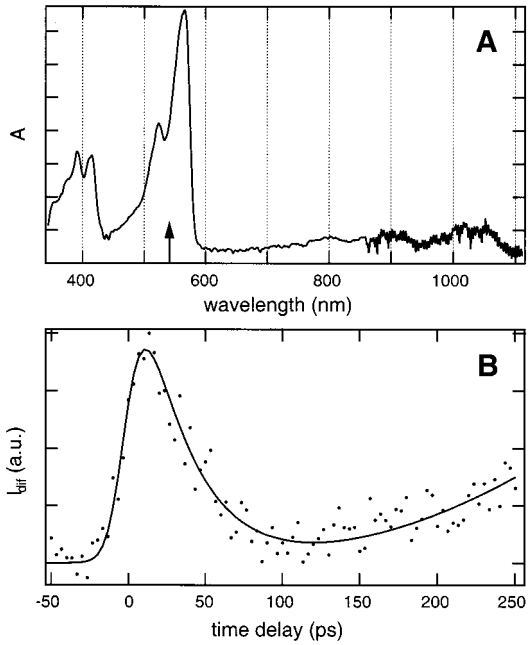

Figure 4. (A) Absorption spectrum of $AQ^{\bullet-}$ in MTHF (small arrow: pump and probe wavelength) and (B) Time profile of the diffracted intensity at 532 nm and best fit (see text).

ET process, but can be due to an ultrafast charge recombination (CR) in the resulting ion pair. If the CR is much faster than the forward ET quenching, the dication population remains very small and might therefore be difficult to detect. In addition, the 660 nm band observed in the TG spectrum of $TE^{\bullet+}$ (Figure 2C) and ascribed to $TE^{\bullet+}$* may hide the presence of TE^{2+}, which also absorbs in this region. In some cases, CR of ion pairs can take place in less than 1 ps.[25]

It is well-known that pure sulfuric acid is not a single substance, but comprises a dynamic equilibrium involving several species.[58] Therefore, the exact mechanism of the photoinduced ET in this medium is difficult to establish. The second oxidation potential of PE and TE in ACN is about 0.5 V above the first one ($E_{ox}(PE^{\bullet+}) = 1.59$ V vs SCE, $E_{ox}(TE^{\bullet+}) = 1.47$ V vs SCE).[59] The oxidation potential of the excited cations can thus be estimated to be equal to 0.09 and 0.07 V, for $PE^{\bullet+}$* and $TE^{\bullet+}$*, respectively, in ACN. Because the formation of $PE^{\bullet+}$ and $TE^{\bullet+}$ is spontaneous in H_2SO_4, the oxidation of the cations in their first excited state should therefore be energetically possible. The markedly higher oxidation potential of $TH^{\bullet+}$*, ($E_{ox}(TH^{\bullet+}) \approx 0.35$ V),[40] could explain why such a bimolecular quenching mechanism is not operative with this species. The isotope effects on ET quenching and CR reactions are known to be small ($\tau_D/\tau_H < 2$),[60−62] in agreement with those reported above.

A photoinduced ET process could also be at the origin of the short lifetime of $PE^{\bullet+}$* in ACN.[16] In this case, $PE^{\bullet+}$ was formed by ET between PE* and TCNE. TCNE is a strong acceptor ($E_{red} = +0.24$ V vs SCE)[63] and hence the reaction $PE^{\bullet+}$* + TCNE → PE^{2+} + $TCNE^{\bullet-}$ is energetically favorable ($\Delta G_{ET} = -0.15$ eV). The CR process is not highly exergonic ($\Delta G_{CR} = -1.4$ eV) and can therefore be expected to occur close to the barrierless regime and to be consequently ultrafast.[25] A reinvestigation of the excited dynamics of radical cations formed by photoinduced ET using a better time resolution is planned.

Radical Anions. *Anthraquinone Radical Anion.* The radical anion of anthraquinone, $AQ^{\bullet-}$, was prepared by γ irradiation in a MTHF glass. The resulting absorption spectrum is shown in Figure 4A and is identical to those reported in the litera-

ture.[38,64] The excited-state lifetime of this anion was determined from TG measurements of the GSR dynamics at 532 nm (see Figure 4B). The diffracted intensity decays to a value close to zero before increasing again. This increase is caused by the build up of a density phase grating due to thermal expansion.[65,66] Indeed, if part of the excitation energy is converted into heat through a nonradiative process, the temperature becomes spatially modulated and a transient density phase grating is formed. The build-up time of this grating is approximately the sum of the time constant of the heat releasing process and of half the acoustic period,[66] which was around 2 ns in this experiment. The continuous line in Figure 4B is the best fit of the eq 3 in ref 67, valid for mixed gratings.

The initial decay of the TG intensity to a value close to zero indicates that photobleaching of $AQ^{\bullet-}$ is not efficient. Electron photoejection is known to be a major deactivation pathway of excited radical anions in the gas phase or in nonpolar solvents.[68] The threshold energy for electron ejection of $AQ^{\bullet-}$ amounts to 1.6 and 3.5 eV in the gas phase and in ACN, respectively.[16] The fact that this process does not take place in a MTHF glass with 2.33 eV irradiation is certainly due to the stabilization of $AQ^{\bullet-}$ by the matrix. Using the Born equation and a value of 2 for the dielectric constant of glassy MTHF, the solvation energy of an anion of the size of $AQ^{\bullet-}$ is around 1 eV, resulting in a threshold energy for photoejection of about 2.6 eV (475 nm). The analysis of the time profile of the diffracted intensity shown in Figure 4B results in an $AQ^{\bullet-}$* lifetime of 70 ps. This is much shorter than the lifetime reported for other excited anions,[11,15] but substantially longer than that the upper limit of 15−20 ps found for $AQ^{\bullet-}$* generated by photoinduced ET of AQ* with DABCO in ACN.[16] Upon laser excitation at 532 nm, the sample exhibits a weak emission around 570 nm. This band is not due to fluorescence of $AQ^{\bullet-}$*, because the same emission can be obtained with the sample before γ irradiation and it is also measured when exciting the nonirradiated sample at 355 nm. In this case, however, more bands with a higher intensity can be observed at shorter wavelength. This spectrum can be safely ascribed to the phosphorescence of ^{3}AQ*.[69] The observation of a single band at 570 nm, when exciting at 532 nm, can be explained by the presence of a 550 nm cutoff filter in front of the spectrograph. The phosphorescence on 532 nm excitation is probably due to two-photon absorption of AQ. Apart from this 570 nm band, no emission that could be ascribed to $AQ^{\bullet}$* was observed below 1000 nm.

Tetracenequinone Radical Anion. Alkali metals have been known for a long time to react with aromatic hydrocarbons in suitable solvents to yield radical anions.[70] This procedure has been applied here to generate the radical anion of tetracenequinone, $TQ^{\bullet-}$. After mixing of neutral TQ with potassium in dry and deoxygenated THF, a red solution was obtained. The absorption spectrum of this solution consists of a band with a maximum at 525 nm with a shoulder at 560 nm (see Figure 5). Upon excitation at 532 nm, this species exhibits a weak emission with a maximum around 620 nm and a lifetime of 1.45 ns. As shown in Figure 5, the excitation spectrum of the 620 nm band is very similar to the absorption spectrum.

To check whether this emitting species is really $TQ^{\bullet-}$, this anion was also generated by photoinduced ET between TQ* and DABCO. As ET takes place from ^{3}TQ*, the ensuing geminate ion pair is in a triplet state, hence the geminate charge recombination is spin forbidden and the separation efficiency of the ion pair to free ions is essentially unity.[64,71]

Figure 6A shows the TG spectrum obtained 1 ns after excitation of a solution of TQ with 0.1 M DABCO in ACN.

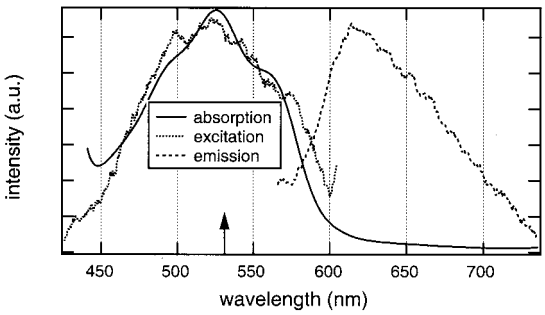

Figure 5. Absorption, emission and excitation spectra measured with a solution of TQ dissolved with K in THF (small arrow: pump wavelength).

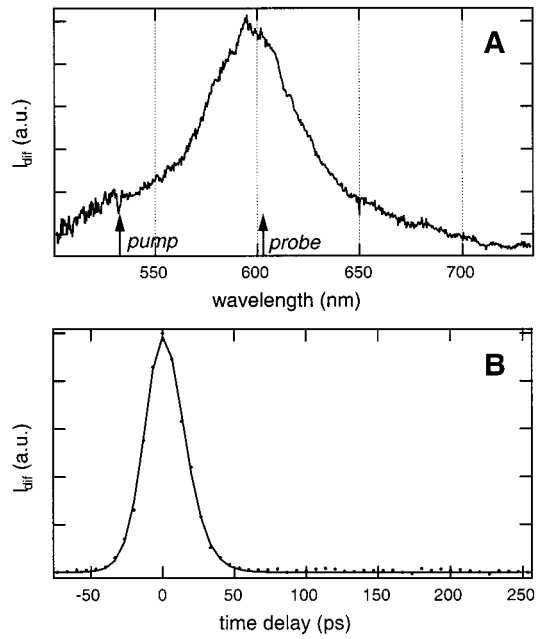

Figure 6. (A) TG spectrum measured 1 ns after excitation at 355 nm of TQ with 0.1 M DABCO in ACN (small arrows: pump and probe wavelengths). (B) Time profile of the diffracted intensity at 604 nm measured with $TQ^{\bullet-}$ in ACN after excitation at 532 nm and best fit of eq 1.

The maximum of the TG band is centered at 590 nm, rather far from the absorption band measured in THF. The excited-state lifetime of $TQ^{\bullet-}$ in ACN was determined using the technique described in detail in ref 16. Briefly, 7 ns after excitation of the TQ/DABCO solution at 355 nm, a TG grating experiment was performed on the resulting $TQ^{\bullet-}$ population. The grating was formed by exciting the $TQ^{\bullet-}$ population with two 532 nm pulses, and the GSR dynamics was probed with a third pulse at 604 nm, generated by Raman shifting the 532 nm pulses in ACN. The measured time profile of the diffracted intensity is shown in Figure 6B. This profile cannot be differentiated from the third-order autocorrelation function of the laser pulses, indicating that the GSR of $TQ^{\bullet-}$ in ACN is shorter than about 20 ps. The diffracted signal is clearly due to the $TQ^{\bullet-}$ population, because it vanishes on blocking the 355 nm actinic pulse.

This short GSR time of $TQ^{\bullet-}$ differs completely from the fluorescence lifetime measured with TQ/K in THF, supporting the assumption that the species emitting in THF/K is not $TQ^{\bullet-}$. No emission that could be ascribed to $TQ^{\bullet-}$* was detected with the system TQ/DABCO in ACN.

$TQ^{\bullet-}$ was also generated by γ irradiation in an MTHF glass at 77 K. The spectrum of such a sample is shown in Figure 7 and consists of a band with a maximum at 610 nm and a

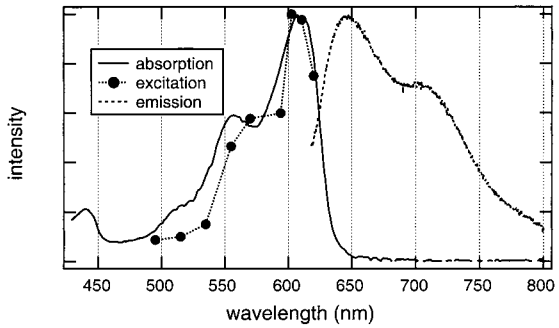

Figure 7. Absorption, emission, and excitation spectra measured with $TQ^{\bullet-}$ in a MTHF glass at 77 K.

shoulder at 560 nm. This spectrum agrees quite well with the TG spectrum measured with TQ/DABCO in ACN, and supports further the assumption that the emitting species formed in THF/K is not $TQ^{\bullet-}$, but probably a secondary product, as it is often the case with radical ions in solution.[8] An ion pairing effect cannot be invoked to account for the spectral differences observed with TQ/K in THF and TQ/DABCO in ACN or $TQ^{\bullet-}$ in MTHF glass. If this were the case, the absorption spectrum of $TQ^{\bullet-}$ in THF should depend on the nature of the counterion, as observed with many radical anions of aromatic ketones.[72] However, going from TQ/K to TQ/Na in THF has no influence on the resulting absorption spectra.

The GSR dynamics of $TQ^{\bullet-}$ in MTHF glass could not be determined, because of the weak absorbance at 532 nm and the poor optical quality of the glass. However, a weak emission could clearly be measured. As shown in Figure 7, the emission band has its maximum at 650 nm with a shoulder at 700 nm and is a rather good mirror image of the absorption band of $TQ^{\bullet-}$. The phosphorescence spectrum of neutral TQ was measured upon excitation at 355 nm of TQ in a nonirradiated MTHF glass. It consists of three main bands with maxima at 511, 552, and 596 nm. The emission band shown in Figure 7 is therefore not due to neutral TQ. To ascribe univocally the origin of this emission, its excitation spectrum was recorded. The black circles in Figure 7 are the intensities of the 650 nm emission band recorded at different wavelengths of the OPO used for excitation. The resulting spectrum matches rather closely the absorption band of $TQ^{\bullet-}$, confirming that the 620 nm emission is due to $TQ^{\bullet-}$*. The small difference between the excitation and the absorption spectra could be due to a spatial variation of the OPO pulse shape with the wavelength. The fluorescence quantum yield was estimated to be of the order 10^{-3} and the lifetime was shorter than the resolution of the time-resolved fluorescence system.

Fluorescence from radical anions in low-temperature matrices has already been reported for 1,4-benzoquinone[11] and for some chalcone derivatives.[15] In the first case, the fluorescence lifetime is 63 ns and the quantum yield 0.003. The large natural fluorescence lifetime of this anion was ascribed to the forbidden nature of the D_1-D_0 transition.[11] The fluorescence quantum yields of the chalcone anions is very small and the lifetimes range between 1 and 3 ns.[15] These emissions originate from the lowest doublet excited states of the anions. The situation is apparently different with $TQ^{\bullet-}$.

Table 3 shows the excited-state energies of $TQ^{\bullet-}$ together with the oscillator strengths for the corresponding transitions from ground-state $TQ^{\bullet-}$. The calculations show that the 610 nm absorption band is not due to the first electronic transition of $TQ^{\bullet-}$, but rather to the D_0-D_3 or to the D_0-D_2 transition, both D_2 and D_3 being close to each other. The D_1 state is at much lower energy and the corresponding D_0-D_1 absorption band should appear around 1630 nm. The absence of this band in the experimental absorption spectrum of $TQ^{\bullet-}$ agrees with the very small oscillator strength calculated for this transition. These data imply that the 650 nm emission band ascribed to $TQ^{\bullet-}$* originates from an upper excited state.

TABLE 3: Calculated Vertical Energies of the First Five Excited States of $TQ^{\bullet-}$ and Oscillator Strengths *f* for Transition from the $^2A_2$ Ground State to these States or vice versa

state symmetry	energy (eV)	wavelength (nm)	f
$^2A_2$	(0)	–	
$^2B_1$	0.759	1633	0.0049
$^2B_1$	2.056	603	0.0028
$^2A_2$	2.180	569	0.2019
$^2B_2$	2.519	492	0.0000
$^2B_1$	2.549	486	0.0013

Because of the proximity of the D_3 and D_2 states, the emission must certainly occur from D_2. The calculations predict a very low oscillator strength for electronic transition between the ground state and D_2, but a large one for D_3, which lies only 0.12 eV above. Consequently, the emitting D_2 state must certainly correspond to the calculated D_3 state. The TD-B3LYP method is not expected to give predictions to an accuracy below the D_3/D_2 splitting, and the effect of the environment, which is not taken into account in the calculations, could exacerbate the small difference between the experiment and the calculations.

Emission from an upper excited state of $TQ^{\bullet-}$ is not really surprising if one considers the wide D_2-D_1 energy gap, which is even larger than the D_1-D_0 gap, and the large oscillator strength of the D_2-D_0 transition. Therefore, emission from an upper excited state can compete with IC, as it is also the case with azulene derivatives,[73] aromatic thioketones,[74] and several porphyrins.[75] Equation 2 predicts a natural fluorescence lifetime of 12 ns for the D_2-D_0 transition of $TQ^{\bullet-}$, while eq 3 indicates an IC time constant of 50 ps. The resulting fluorescence quantum yield of about 4×10^{-3} is in reasonable agreement with our estimate.

For $AQ^{\bullet-}$*, the D_2-D_1 energy gap is certainly too small to observe emission from D_2. An oscillator strength of 0.07 can be estimated for the D_0-D_2 transition, using an absorption coefficient of 8000 cm^{-1} M^{-1} for the band maximum.[76] The resulting natural fluorescence lifetime amounts to about 30 ns. The D_2-D_1 energy gap is small and thus the decay of D_2 via IC should occur with a time constant of 14 ps. Therefore, the D_2-D_0 fluorescence of $AQ^{\bullet-}$*, whose quantum yield should not exceed 4×10^{-4}, should be very difficult to observe experimentally. Emission from D_1 should be equally problematic to detect, because of a fast IC ($\tau_{IC} \approx 50$ ps), in accord with the GSR time constant of 70 ps, of the small oscillator strength of the D_1-D_0 transition, and of the spectral region of the emission.

Conclusion

The results show that the excited state lifetimes of organic radical ions depend strongly on the environment. In liquid solutions, the occurrence of intermolecular quenching processes shortens the lifetime substantially. The mechanism of these quenching processes is still not clear but most probably involves a reversible charge transfer reaction. This deactivation channel is not operative in low-temperature matrices and thus the excited state lifetime is substantially longer.

It was also shown that the absence of a low lying excited state is not a prerequisite for the observation of fluorescence from an excited radical ion. The really important parameters

are a large oscillator strength for the transition and a large energy gap between the emitting state and the next lower state. Such conditions are met with $TQ^{\bullet-}$ but not with $AQ^{\bullet-}$ and $TH^{\bullet+}$, and therefore, only the first ion fluoresces significantly in the visible.

Many more measurements with a large set of molecules and with a very high time resolution are required for a better understanding of the excited-state dynamics of radical ions in the condensed phase.

Acknowledgment. We thank Mr. J. -L. Roulin for the purification of many compounds. This work was supported by the Fonds national suisse de la recherche scientifique through Projects 2000-055388.98 and 2000-061560.00.

References and Notes

(1) Jortner, J., Bixon, M., Eds. *Electron transfer: from isolated molecules to biomolecules*; J. Wiley: New York, 1999; Vol. 106.

(2) Hug, G. L.; Marciniak, B. *J. Phys. Chem.* **1995**, *99*, 1478.

(3) Schmidt, G. D.; Cohen, M.; Margon, B. *Astrophys. J.* **1980**, *239*, L133.

(4) Moutet, J.-C.; Reverdy, G. *Nouv. J. Chem.* **1983**, *7*, 105.

(5) Shine, H.; Zhao, D.-C. *J. Org. Chem.* **1990**, *55*, 4086.

(6) Miller, T. A. *Annu. Rev. Phys. Chem.* **1982**, *33*, 257.

(7) Klapstein, D.; Maier, J. P.; Misev, L. In *Molecular Ions: Spectroscopy, Structure and Chemistry*; Miller, T. A., Bondybey, V. E., Eds.; North-Holland: Amsterdam, 1983; p 175.

(8) Breslin, D. T.; Fox, M. A. *J. Phys. Chem.* **1994**, *98*, 408.

(9) Joblin, C.; Salama, F.; Allamandola, L. *J. Chem. Phys.* **1995**, *102*, 9743.

(10) Pankasem, S.; Iu, K. K.; Thomas, J. K. *J. Photochem. Photobiol. A* **1991**, *62*, 53.

(11) Cook, A. R.; Curtiss, L. A.; Miller, J. R. *J. Am. Chem. Soc.* **1997**, *119*, 5729.

(12) Zimmer, K.; Hoppmeier, M.; Schweig, A. *Chem. Phys. Lett.* **1998**, *293*, 366.

(13) Zimmer, K.; Gödicke, B.; Hoppmeier, M.; Meyer, H.; Schweig, A. *Chem. Phys.* **1999**, *248*, 263.

(14) Ichinose, N.; Tanaka, T.; Kawanishi, S.; Suzuki, T.; Endo, K. *J. Phys. Chem. A* **1999**, *103*, 7923.

(15) Hiratsuka, H.; Yamazaki, T.; Maekawa, Y.; Kajii, Y.; Hikida, T.; Mori, Y. *Chem. Phys. Lett.* **1987**, *139*, 187.

(16) Gumy, J.-C.; Vauthey, E. *J. Phys. Chem. A* **1997**, *101*, 8575.

(17) Gumy, J. C.; Nicolet, O.; Vauthey, E. *J. Phys. Chem. A* **1999**, *103*, 10737.

(18) Domcke, W.; Stock, G. *Adv. Chem. Phys.* **1997**, *100*, 1.

(19) Wurzer, A. J.; Wilhelm, T.; Piel, J.; Riedle, E. *Chem. Phys. Lett.* **1999**, *299*, 296.

(20) Bearpark, M. J.; Bernardi, F.; Clifford, S.; Olivucci, M.; Robb, M. A.; Smith, B. R.; Vreven, T. *J. Am. Chem. Soc.* **1996**, *118*, 169.

(21) Högemann, C.; Pauchard, M.; Vauthey, E. *Rev. Sci. Instrum.* **1996**, *67*, 3449.

(22) Vauthey, E. *J. Phys. Chem. A* **1997**, *101*, 1635.

(23) Högemann, C. Ph.D. Thesis, University of Fribourg, 1999.

(24) Gumy, J.-C. Ph.D. Thesis, University of Fribourg, 2000.

(25) Vauthey, E. *J. Phys. Chem. A* **2001**, *105*, 340.

(26) Perrin, D. D.; Armarego, W. L. F.; Perrin, D. R. *Purification of Laboratory Chemicals*; Pergamon Press: Oxford, 1980.

(27) Shida, T.; Haselbach, E.; Bally, T. *Acc. Chem. Res.* **1984**, *17*, 180.

(28) Sarbach, A. Ph.D. Thesis, University of Fribourg, 2000.

(29) Kimura, K.; Yamazaki, T.; Katsumata, S. *J. Phys. Chem.* **1971**, *75*, 1768.

(30) Hübler, P.; Jürgen, H. *Ber. Bunsen-Ges. Phys. Chem.* **1998**, *102*, 1506.

(31) Becke, A. D. *J. Chem. Phys.* **1993**, *98*, 5648.

(32) Lee, C.; Yang, W.; Parr, R. G. *Phys. Rev. B* **1988**, *37*, 785.

(33) Frisch, M. J.; Trucks, G. W.; Schlegel, H. B.; Scuseria, G. E.; Robb, M. A.; Cheeseman, J. R.; Zakrzewski, V. G.; Montgomery, J. A.; Stratmann, R. E.; Burant, J. C.; Dapprich, S.; Millam, J. M.; Daniels, A. D.; Kudin, K. N.; Strain, M. C.; Farkas, O.; Tomasi, J.; Barone, V.; Cossi, M.; Cammi, R.; Mennucci, B.; Pommelli, C.; Adamo, C.; Clifford, S.; Ochterski, J.; Petersson, G. A.; Ayala, P. Y.; Cui, Q.; Morokuma, K.; Malick, D. K.; Rabuck, A. D.; Raghavachari, K.; Foresman, J. B.; Cioslowski, J.; Ortiz, J. V.; Stefanov, B. B.; Liu, G.; Liashenko, A.; Piskorz, P.; Komaromi, I.; Gomperts, R.; Martin, R. L.; Fox, D. J.; Keith, T.; Al-Laham, M. A.; Peng, C. Y.; Nanayakkara, A.; Challacombe, M.; Gill, P. M. W.; Johnson, B. G.; Chen, W.; Wong, M. W.; Andres, J. L.; Gonzales, C.; Head-Gordon, M.; Repogle, E. S.; Pople, J. A. *Gaussian 98*, Revision A1; Gaussian, Inc.: Pittsburgh, PA, 1998.

(34) Johnson, B. G.; Gill, P. M. W.; Pople, J. A. *J. Chem. Phys.* **1993**, *98*, 5612.

(35) Casida, M. E. In *Recent Advances in Density Functional Methods, Part I*; Chong, D. P., Ed.; World Scientific: Singapore, 1995; p 155.

(36) Stratmann, R. E.; Scuseria, G. E.; Frisch, M. J. *J. Chem. Phys.* **1998**, *109*, 8218.

(37) The transition moments that appear in the TD-DFT output of Gaussian should probably be taken with a grain of salt, because their absolute values vary by orders of magnitude depending on the number of excited states (NStates=nn) that are calculated.

(38) Shida, T. *Electronic Absorption Spectra of Radical Ions*; Physical Sciences Data 34; Elsevier: Amsterdam, 1988..

(39) Aalbersberg, W. I.; Hoijtink, G. J.; Mackor, E. L.; Weiland, W. P. *J. Chem. Soc.* **1959**, 3049.

(40) Bock, H.; Rauschenbach, A.; Noether, C.; Kleine, M.; Havlas, Z. *Chem. Ber.* **1994**, *127*, 2043.

(41) Kogelnik, H. *Bell Syst. Tech. J.* **1969**, *48*, 2909.

(42) Joo, T.; Jia, Y.; Yu, J.-Y.; Lang, M. J.; Fleming, G. R. *J. Chem. Phys.* **1996**, *104*, 6089.

(43) Goldberg, S. Y.; Bart, E.; Meltsin, A.; Fainberg, B. D.; Huppert, D. *Chem. Phys.* **1994**, *183*, 217.

(44) Deeg, F. W.; Fayer, M. D. *J. Chem. Phys.* **1989**, *91*, 2269.

(45) Högemann, C.; Vauthey, E. *Isr. J. Chem.* **1998**, *38*, 181.

(46) Turro, N. J. *Modern Molecular Photochemistry*; University Science Book: Sausalito, 1991.

(47) Siebrand, W.; Williams, D. F. *J. Chem. Phys.* **1968**, *49*, 1860.

(48) Tominaga, K.; Kliner, D. A.; Johnson, A. E.; Levinger, N. E.; Barbara, P. F. *J. Chem. Phys.* **1993**, *98*, 1228.

(49) Miyasaka, H.; Hagihara, M.; Okada, T.; Mataga, N. *Chem. Phys. Lett.* **1992**, *188*, 259.

(50) Laermer, F.; Elsaesser, T.; Kaiser, W. *Chem. Phys. Lett.* **1989**, *156*, 381.

(51) Siebrand, W.; Williams, D. F. *J. Chem. Phys.* **1967**, *46*, 403.

(52) Shkrob, I. A.; Sauer, M. G., Jr.; Liu, A. D.; Crowell, R. A.; Trifunac, A. D. *J. Phys. Chem. A* **1998**, *102*, 4976.

(53) Aalbersberg, W. I.; Hoijtink, G. J.; Mackor, E. L.; Weiland, W. P. *J. Chem. Soc.* **1959**, 3055.

(54) Stevens, C. G.; Strickler, S. J. *J. Am. Chem. Soc.* **1973**, *95*, 3922.

(55) Shizuka, H.; Tobita, S. *J. Am. Chem. Soc.* **1982**, *104*, 6919.

(56) Snoek, L. C.; Clement, S. G.; Harren, F. J. M.; Zande, W. J. v. d. *Chem. Phys. Lett.* **1996**, *258*, 461.

(57) Brouwer, D. M.; vanDoorn, J. A. *Rec. Trav. Chim.* **1972**, *91*, 1110.

(58) Greenwood, N. N.; Earnshaw, A. *Chemistry of the Elements*; Pergamon Press: Oxford, 1985.

(59) Kubota, T.; Kano, K.; Uno, B.; Konse, T. *Bull. Chem. Soc.* **1987**, *60*, 3865.

(60) Pal, H.; Nagasawa, Y.; Tominaga, K.; Yoshihara, K. *J. Phys. Chem.* **1996**, *100*, 11964.

(61) Muller, P.-A.; Högemann, C.; Allonas, X.; Jacques, P.; Vauthey, E. *Chem. Phys. Lett.* **2000**, *236*, 321.

(62) Dresner, J.; Prochorow, J. *Chem. Phys. Lett.* **1978**, *54*, 292.

(63) Mataga, N.; Kanda, Y.; Asahi, T.; Miyasaka, H.; Okada, T.; Kakitani, T. *Chem. Phys.* **1988**, *127*, 239.

(64) Haselbach, E.; Vauthey, E.; Suppan, P. *Tetrahedron* **1988**, *44*, 7335.

(65) Nelson, K. A.; Casalegno, R.; Miller, R. J. D.; Fayer, M. D. *J. Chem. Phys.* **1982**, *77*, 1144.

(66) Vauthey, E.; Henseler, A. *J. Photochem. Photobiol. A* **1998**, *112*, 103.

(67) Brodard, P.; Vauthey, E. *Chem. Phys. Lett.* **1999**, *309*, 198.

(68) Bondybey, V. E.; Miller, T. A. In *Molecular Ions: Spectroscopy, Structure and Chemistry*; Miller, T. A., Bondybey, V. E., Eds.; North-Holland: Amsterdam, 1983; p 125.

(69) Kuboyama, A.; Matzusaki, S. Y. *Bull. Chem. Soc. Jpn.* **1981**, *54*, 3635.

(70) Balk, P.; Hoijtink, G. J.; Schreurs, J. W. H. *Rec. Trav. Chim.* **1957**, *76*, 813.

(71) Pilloud, D. Ph.D. Thesis, University of Fribourg, 1993.

(72) Carter, H. V.; McClelland, B. J.; Warhurst, E. *Trans. Faraday Soc.* **1960**, *56*, 455.

(73) Beer, M.; Longuet-Higgins, H. C. *J. Chem. Phys.* **1955**, *23*, 1390.

(74) Maciejewski, A.; Steer, R. P. *Chem. Rev.* **1993**, *93*, 67.

(75) Kalyanasundaram, K. *Photochemistry of Polypyridine and Porphyrin Complexes*; Academic Press: San Diego, 1992.

(76) Högemann, C.; Vauthey, E. *J. Phys. Chem. A* **1998**, *102*, 10051.